FINITE ELEMENT COMPUTATION OF A TURBULENT FLOW OVER A TWO-DIMENSIONAL BACKWARD-FACING STEP

A. AUTRET AND M. GRANDOTTO

Centre d'Etudes Nucléaires de Cadarache, DRE/STRE/LMA, F-13108 St Paul lez Durance Cedex, France

AND

I. DEKEYSER

Institut de Mécanique Statistique de la Turbulence, Unité Associée au C. N. R. S. numéro 130,
12 Avenue Général Leclerc, F-13003 Marseille, France

SUMMARY

This paper is devoted to the computation of turbulent flows by a Galerkin finite element method. Effects of turbulence on the mean field are taken into account by means of a k–ε turbulence model. The wall region is treated through wall laws and, more specifically, Reichardt's law. An inlet profile for ε is proposed as a numerical treatment for physically meaningless values of k and ε. Results obtained for a recirculating flow in a two-dimensional channel with a sudden expansion in width are presented and compared with experimental values.

KEY WORDS k–ε Turbulence model   Galerkin Finite Element Method   Penalty Function Approach   Wall Law   Backward-Facing Step

INTRODUCTION

The accurate prediction of the behaviour of a turbulent flow in complex geometries is the basic task of hydraulicians in the nuclear sphere. Accuracy is a very important feature of a numerical model which consists of a turbulence model and a computational method. For example, the failure to predict the existence of a recirculating zone or the precise location of a reattachment point could have dramatic consequences on the performance of a mechanical system.

With respect to the computational method a great deal of attention has been given in recent years by many researchers to the finite element method.[1,2] Specifically, the Galerkin finite element method associated with a penalty function approach has been shown to be very accurate for solving the Navier–Stokes equations.

In the context of turbulent flows the task is more difficult insofar as it is necessary to use a turbulence model to describe the physical behaviour of the fluid. The model consists of a set of partial differential equations, algebraic relations and boundary conditions. The main expected aim is to correctly depict the spatial variation of the effective dynamic viscosity which is necessary for solving the momentum equations. This can be achieved by implementing models comprising zero, one, two or more equations.

The present paper deals with the numerical computation of a turbulent flow by way of a two-equation model using one partial differential equation for the turbulent kinetic energy and another for the turbulent energy dissipation rate. The closure of this set of partial differential equations is then performed by algebraic relations. It will be shown how this standard turbulence model cannot account for all physical situations. Moreover, the mean field is not very well predicted when the model is used in dissociation from physical considerations.

THEORETICAL BASIS—TURBULENCE MODEL

The classical Navier–Stokes equations for a viscous, incompressible, steady, Newtonian, isothermal, two-dimensional flow, with external forces neglected, can be written as

$$\rho U_j U_{i,j} = (f_{ij} - \rho \overline{u_i u_j})_{,j},$$ (1)

$$U_{i,i} = 0,$$ (2)

in which $\{i,j\} = \{1,2\}$ and repeated indices require summation, U_i denotes the component of the mean velocity in the x_ith co-ordinate direction of a Cartesian system (x_1, x_2), ρ is the density and f_{ij} is the mean viscous shear stress tensor defined by

$$f_{ij} = -P\delta_{ij} + \mu(U_{i,j} + U_{j,i}),$$ (3)

where P denotes the mean pressure, δ_{ij} the Kronecker symbol and μ the molecular viscosity. The quantities μ and ρ are assumed to be constant.

The turbulent Reynolds shear stress $\overline{\rho u_i u_j}$ (the overbar denotes a time average) is often connected to the mean field by means of the generalized Boussinesq hypothesis

$$-\rho \overline{u_i u_j} = \mu_T(U_{i,j} + U_{j,i}) - \tfrac{2}{3}\rho k \delta_{ij},$$ (4)

in which μ_T is the dynamic eddy viscosity and

$$k = \tfrac{1}{2}\overline{u_i^2}$$ (5)

is the turbulent kinetic energy.

Introducing the new variable

$$P^* = P + \tfrac{2}{3}\rho k$$ (6)

and employing (4), equation (1) can be written

$$\rho U_j U_{i,j} = T_{ij,j},$$ (7)

where

$$T_{ij} = -P^*\delta_{ij} + \mu_e(U_{i,j} + U_{j,i})$$ (8)

with

$$\mu_e = \mu + \mu_T$$ (9)

the effective dynamic viscosity.

In the present paper, following Jones and Launder[3] and nearly all subsequent workers, μ_T will be expressed in terms of the turbulent kinetic energy k and the turbulent energy dissipation rate ε via the relation

$$\mu_T = c_\mu \rho k^2 / \varepsilon.$$ (10)

The two variables k and ε are deduced from their own transport equations:[3]

$$\rho U_j k_{,j} = \left[\left(\mu + \frac{\mu_T}{\sigma_k} \right) k_{,j} \right]_{,j} + \mu_T S - c_D \rho \frac{k^{3/2}}{L},$$ (11)

$$\rho U_j \varepsilon_{,j} = \left[\left(\mu + \frac{\mu_T}{\sigma_\varepsilon} \right) \varepsilon_{,j} \right]_{,j} + c_{1\varepsilon} c_\mu \rho k S - c_{2\varepsilon} \rho \frac{k^2}{\varepsilon},$$ (12)

in which L denotes the turbulent length scale defined by

$$L = c_D (k^{3/2}/\varepsilon)$$ (13)

and S is the term

$$S = U_{i,j} (U_{i,j} + U_{j,i}).$$ (14)

In the set of equations (10)–(13) the quantities σ_k, σ_ε, $c_{1\varepsilon}$, $c_{2\varepsilon}$, c_μ and c_D are considered to be constant. Following Jones and Launder,[3] the values used are 1·00, 1·30, 1·44, 1·92, 0·09 and 1·00 respectively.

Because of the elliptic nature of the system of partial differential equations (1), (2), (11), (12), boundary conditions are required on the whole boundary of the domain. This point will be treated later.

COMPUTATIONAL METHOD

The numerical technique employed to obtain approximate solutions of the system is a standard Galerkin finite element method (GFEM) with a penalty function approach.[4] This last method allows us to take into account the incompressibility condition (2) without explicitly employing Lagrangian multipliers. The pressure values are then recovered from the velocity field by

$$P = -\frac{1}{\lambda} U_{i,i},$$ (15)

in which λ denotes the penalty parameter. Quadrilateral bilinear Lagrangian Q1/PO elements are used for each variable U_i, k and ε with reduced integration of the penalty matrix.[5]

Finally the resulting matrix equations which are to be solved are of the form

$$|\mathbf{C}(U) + \mathbf{D}(\mu_T) + \mathbf{P}| U = F,$$ (16)

$$[\mathbf{C}(U) + (1/\sigma_k)\mathbf{D}(\mu_T) + \mathbf{K}(k, L)] K = \mathbf{P}K(\mu_T, U) U,$$ (17)

$$[\mathbf{C}(U) + (1/\sigma_\varepsilon)\mathbf{D}(\mu_T) + \mathbf{E}(k, \varepsilon)] E = \mathbf{P}E(\mu_T, U) U,$$ (18)

where $\mathbf{C}$ is the matrix of the convective terms, $\mathbf{D}$ is the matrix of the diffusive terms, $\mathbf{P}$ is the penalty matrix, $\mathbf{K}$, $\mathbf{E}$ are the matrices of the dissipative terms and $\mathbf{P}K$, $\mathbf{P}E$ are the matrices of the productive terms. The resolution of the system is performed after linearization of non-linear terms, and the resulting uncoupled structure allows the use of an iterative technique for solving each equation in isolation.[6]

WALL LAWS

The k–ε model equations are elliptic and thus require conditions on the whole boundary $\partial\Omega$ of the mathematical domain of integration Ω. However, in the case of walls it is physically meaningless to integrate the k–ε model equations up to the wall because they are not valid in the vicinity of the

wall. To obviate the necessity to use a modified model in this region of the flow, a fictitious boundary is generally located inside the flow at a distance x_{2p} from the real wall. Then universal laws are used to describe the behaviour of the fluid on this fictitious boundary. This so called wall function method can be obtained by assuming that the near-wall region is in local energy equilibrium so that the non-dimensional velocity profile is logarithmic and the turbulent shear stress is constant. Thus

$$U^+ = \frac{1}{\kappa}(\ln E)x_2^+, \qquad x_2^+ \geqslant 30, \tag{19}$$

in which

$$U^+ = \frac{U}{U_*}, \qquad x_2^+ = \frac{x_2 u_*}{v}, \tag{20}$$

with u_* the friction velocity defined by

$$u_* = \left|\frac{\tau_w}{\rho}\right|^{1/2}, \tag{21}$$

τ_w the wall shear stress, κ the von Karman constant and E the roughness parameter. Usually κ and E are taken to be equal to 0·41 and 9 respectively.

Once u_* is evaluated, near-wall values of k and ε can then be computed from the following relations:[7]

$$k_p = \frac{u_*^2}{c_\mu^{1/2}}, \qquad \varepsilon_p = \frac{u_*^3}{\kappa x_{2p}}. \tag{22}$$

For $x_2^+ < 5$ the following linear law is generally employed:

$$U^+ = x_2^+, \tag{23}$$

whence

$$u_* = \left|\frac{U v}{x_2}\right|^{1/2}. \tag{24}$$

Finally the buffer layer, defined by $5 \leqslant x_2^+ \leqslant 30$, can be taken into account numerically by the datum of some experimental measures or by connecting it with the outer regions.

MODEL SIMULATION

Preliminary computations were performed in a two-dimensional channel with parallel plates and the results were compared with the measurements of Comte-Bellot.[8] Very good agreement was observed for mean and turbulent quantities for three Reynolds numbers.[9] Model simulations were achieved for flow over a two-dimensional backward-facing step. The calculations simulated the experiments of Westphal et al.[10] in which the Reynolds number Re_H, based on the step height, reaches 42000. The geometrical configuration of the flow, the physical data and the boundary conditions imposed for the calculations are depicted in Figure 1.

In the inflow cross-section the U-velocity and k profiles are the experimental ones while the cross-flow velocity V is set to zero. Since there is no satisfactory experimental profile available for ε, an estimated profile has been generated using the following relation,[9] obtained by assuming a
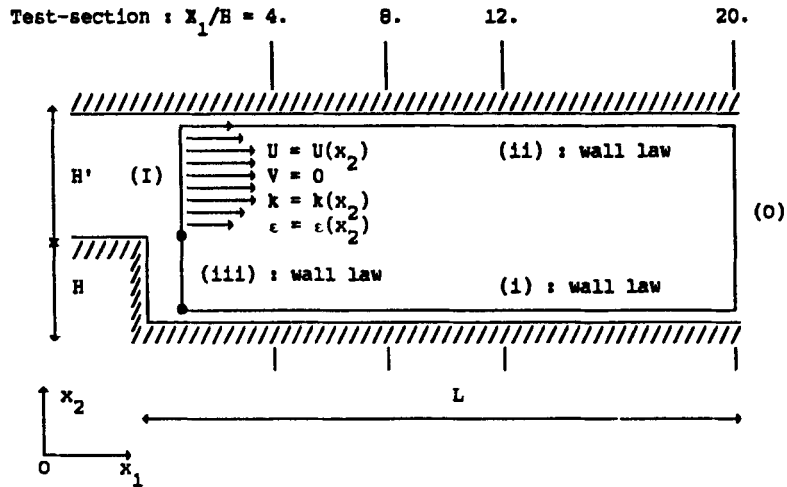
Figure 1

Geometrical data:

$$H = 5 \cdot 08 \text{ cm}; \quad H' = \tfrac{3}{2} H = 7 \cdot 62 \text{ cm}; \quad L = 20 \text{ H} = 1 \cdot 016 \text{ m}$$

$$x_{2_{P(i)}} = 5 \cdot 37 \text{ mm}; \quad x_{2_{P(ii)}} = 3 \cdot 65 \text{ mm}; \quad x_{2_{P(iii)}} = 1 \text{ mm}$$

Physical parameters:

$$\rho = 1 \cdot 208 \text{ kg/m}^3$$

$$\mu = 1 \cdot 437 \ 10^{-5} \text{ kg/ms}$$

Boundary conditions:

* on (I): u, k, ε: experimental values

* on (O): $\dfrac{\partial u}{\partial n} = 0$; $\quad V = 0$; $\quad \dfrac{\partial k}{\partial n} = 0$; $\quad \dfrac{\partial \varepsilon}{\partial n} = 0$

mixing-length hypothesis and a universal logarithmic profile for U:

$$\varepsilon = c_\mu \frac{\kappa x_2 k^2}{L_m^2 u_*}, \tag{25}$$

in which L_m is the Nikuradse mixing-length.

It has been shown[9] that this relation for the ε profile is almost general and can be applied to a large class of problems.

For the outflow cross-section it was assumed:

$$\frac{\partial U}{\partial x_1} = 0, \qquad V = 0, \qquad \frac{\partial k}{\partial x_1} = 0, \qquad \frac{\partial \varepsilon}{\partial x_1} = 0. \tag{26}$$

In the wall region the standard non-dimensional velocity relations (18)–(22) are replaced by Reichardt's law,[11] which can be expanded as

$$U^+ = 2 \cdot 50 \ln(1 + 0 \cdot 40 x_2^+) + 7 \cdot 80 \left(1 - e^{x_2^+/11} - \frac{x_2^+}{11} e^{-0 \cdot 33 x_2^+} \right). \tag{27}$$

The validity of this relation for every positive x_2^+ is the main advantage of this analytical formula in comparison with the standard laws. The relation (27) is treated numerically by a classical fixed-point method accelerated by a fourth-order over-relaxation,[9] giving u_*. However, for $x_2^+ < 2$ the numerical scheme becomes unstable and has to be replaced by the explicit linear law (22). Very small values of x_2^+ could be encountered, for example, near a reattachment point in a recirculating zone. In the two cases the near-wall values of k and ε are then recovered by (22).

Numerical predictions were carried out using a non-uniform mesh employing 27×43 Q1/P0 elements (28×44 nodes). The penalty parameter was equal to 10^6 and about 25–30 fixed-point iterations were necessary to reach the expected convergence criterion (0·5% on each variable U_i, k and ε).

All calculations were performed on a CRAY-XMP computer; about 110 s (CPU time) are sufficient for a complete numerical investigation.

RESULTS

The first attempts were achieved by using the profile of k measured by Westphal *et al.*[10] at the inflow cross-section of the geometrical configuration. Nevertheless, this profile yields a very low turbulence intensity, about 0·3%, on the axis of symmetry in the entrance channel. With this k inlet profile, physically meaningless negative values of k appear in the flow core, emphasizing the non-realizability of the k–ε model. It seems impossible to obviate this difficulty in a natural manner. The onset of negative values of k seems to be connected with small values of the turbulence Reynolds number

$$Re_t = k^2/\nu\varepsilon \tag{28}$$

at the inflow cross-section.

Even a clipping method was not efficient for solving this difficulty. For instance, when the iterative procedure leads to negative values of k they are put to a small preassigned positive quantity; another way of clipping consists of keeping the (positive) values obtained at the previous iteration (see also Betts and Haroutunian[12]). Nevertheless, if the level of k (at the inflow cross-section) is too low, negative values will be always generated by the next iterations. This proves that the k–ε model cannot take into account all physical situations even with realistic boundary conditions. More precisely, it can only reproduce physical configurations in which boundary conditions are consistent with the model itself.

In the present work the profile of k at the inflow cross-section has been replaced by the measured profile of Comte-Bellot[8] obtained in a two-dimensional channel; with this k profile the turbulence Reynolds number is quite similar to the former one except in the vicinity of the axis where the turbulence intensity is significantly higher. With these new conditions the convergence presents no more difficulty but the numerical result downstream of the step differs significantly from experimental results. In particular the experimental reattachment length found by Westphal *et al.*[10] is about 7·33 whereas the numerical estimate is 5·22. This underprediction of the reattachment length by the k–ε model has often been reported.[13, 14] Changing either the inflow section Reynolds number or the inflow section turbulent field did not lead to a more realistic result for the mean field. More generally there is no external action large enough to influence the location of the reattachment point strongly. Numerically it is very clear that the reattachment length depends strongly on the diffusive terms of the momentum equation: the more important they are, the shorter the reattachment length is. The magnitude of these terms was reduced by arbitrarily setting the constant c_μ equal to 0·045. The resulting numerical reattachment length was 7·27, in close agreement with experiment.

A more satisfactory way to solve this problem would be to express c_μ as a function which takes into account local parameters of the turbulence. For example, for thin shear layers Rodi[15] suggested the following dependence of c_μ on the ratio Π/ε, where Π is the production of k:

$$c_\mu = \frac{2}{3}\frac{1-\alpha}{\omega}\frac{1-(1/\omega)(1-\alpha\Pi/\varepsilon)}{[1+(1/\omega)\,(\Pi/\varepsilon-1)]^2},\qquad(29)$$

where α and ω are new constants.

The expression (29) can be deduced from the classical algebraic stress model relations, which are based on the assumption that $\overline{u_1 u_2}/k$ varies only slowly across the flow and that the transport of $\overline{u_1 u_2}$ is proportional to the transport of k.

However, it is very difficult to assign precise values to the new constants. As recommended by Rodi,[15] ω is taken between 2·50 and 2·80 and then α is computed so that c_μ is equal to 0·09 when the flow is in local equilibrium. Corresponding to ω equal to 2·50 and 2·80 are values of α of 0·598 and 0·549 respectively. Corresponding estimates of the reattachment length are 8·33 and 8·53 respectively. Although the estimates are more satisfactory than for a k–ε model with a constant c_μ, the sensitivity of the reattachment length to the change in the constants α and ε is quite high.

COMPARISONS

Comparisons between numerical predictions and experimental profiles have been performed at different test sections located at $x_1/H = 4$, 8, 12 and 20 (Figure 1).

In Figures 2–9 results obtained with $c_\mu = 0\cdot045$ are identified by the letter A, those with $c_\mu = 0\cdot09$ by B and those with a variable c_μ (and $\omega = 2\cdot500$, $\alpha = 0\cdot598$) by C. Experimental results are shown by crosses.

In Figures 10 and 11 the full curves and the crosses represent numerical predictions for $c_\mu = 0\cdot045$ and experimental results respectively.

Velocity profiles

Predictions of the dimensionless longitudinal velocity component U/U_{max} are plotted in Figures 2–5 against the dimensionless ordinate x_2/H, where H is the step height.

For the modified model with $c_\mu = 0\cdot045$ very good agreement can be observed in the recirculating region. Discrepancies become more prominent as the outflow section is approached, but they are relatively easy to try to explain. Downstream of the reattachment point the attached layer assumes the structure of a flat-wall turbulent boundary layer for which a suitable value of the constant c_μ is the standard one. This point is confirmed by the behaviour of the standard model at the last two stations (Figures 4 and 5) in the recovery region. In contrast, the comparison is worse for the upper region.

Finally it can also be observed that the use of relation (29) for c_μ does not improve the outflow cross-section profile very much, even if the predicted location of the maximum is improved.

Turbulent kinetic energy

Comparisons for non-dimensional k profiles are plotted in Figures 6–9.

As in the case of the mean velocity, the predicted maximum values are close to the experimental values. Once more, for the modified model, agreement is good upstream of the reattachment point whereas discrepancies emerge elsewhere. These can be observed in the upper region ($x_2/H > 0\cdot7$), which corresponds to a jet region where the turbulent levels are under-evaluated. It can be seen
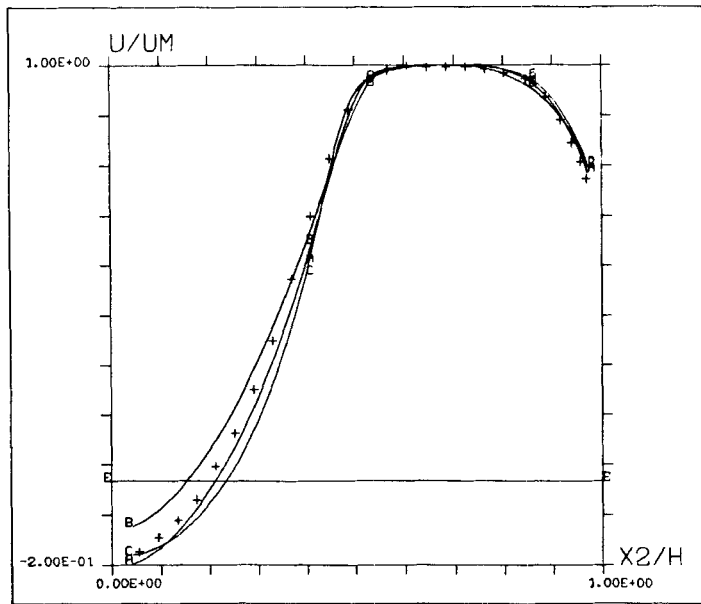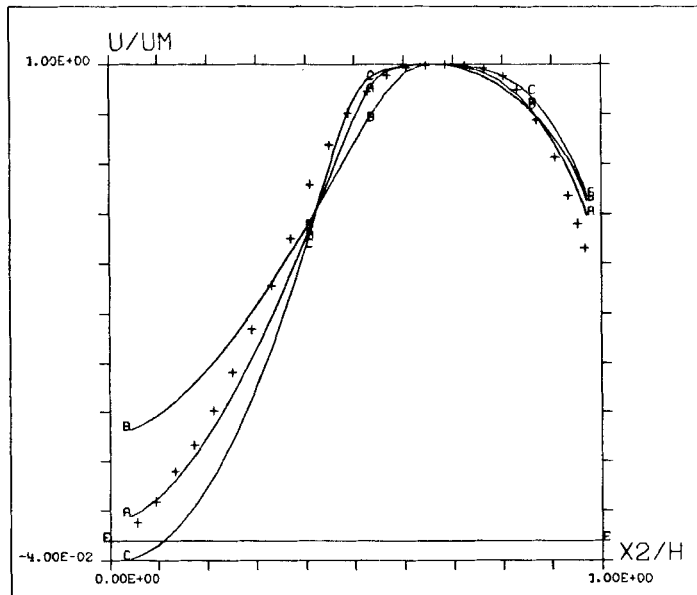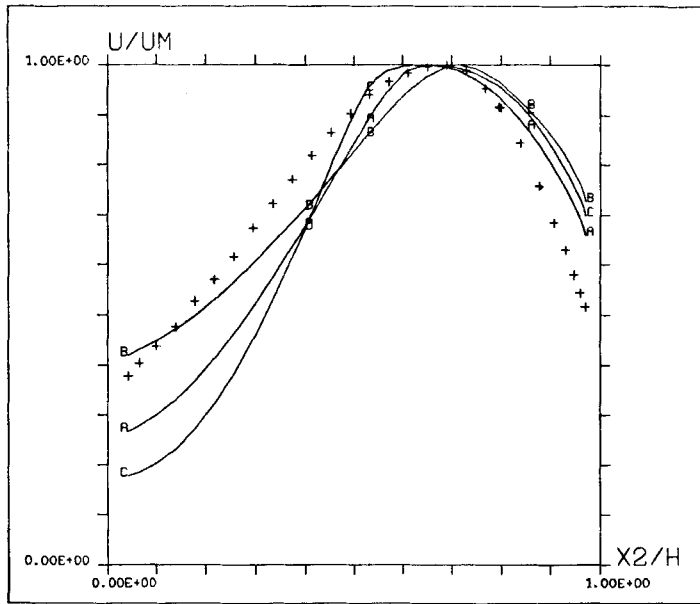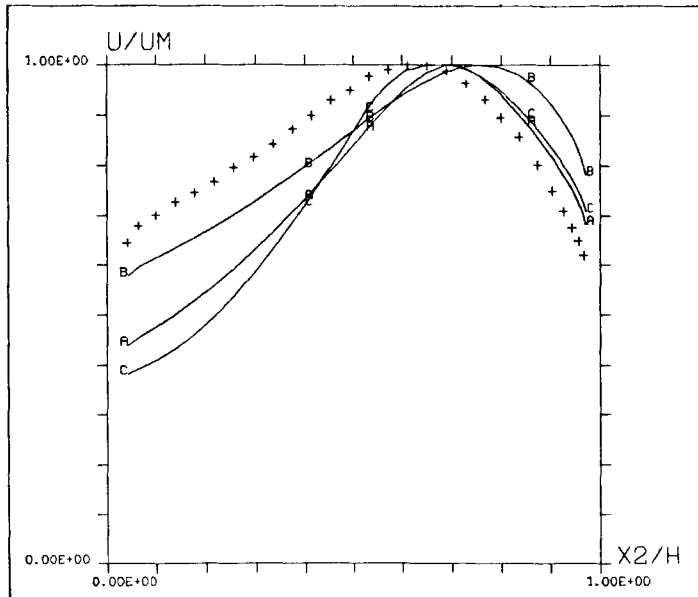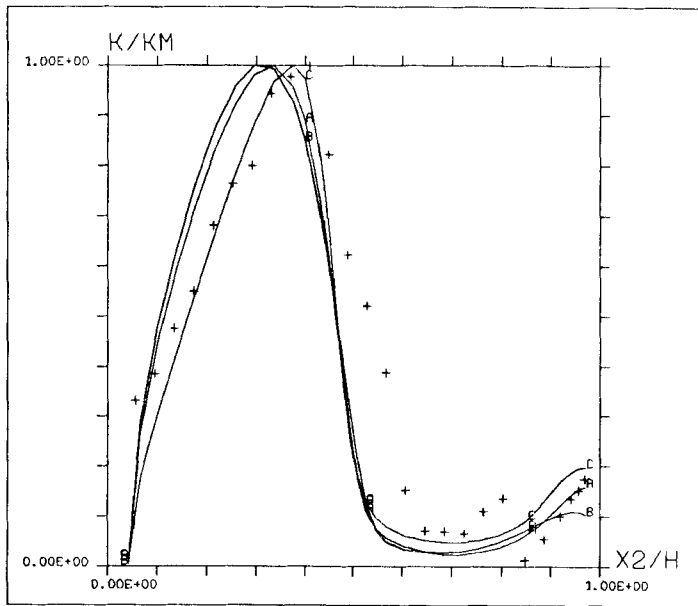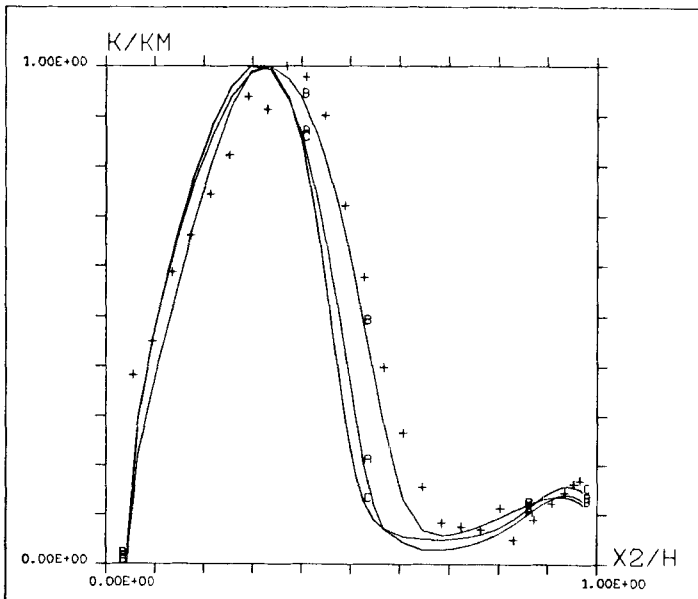
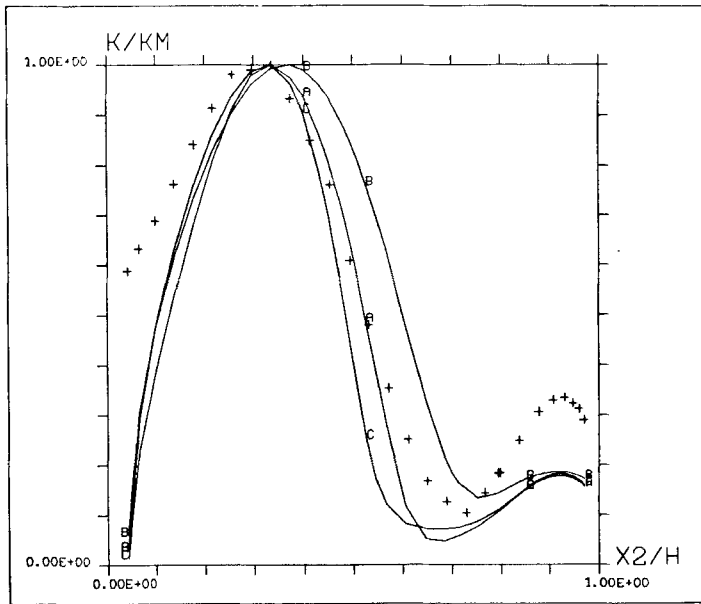Figure 2

Figure 3

Figure 4

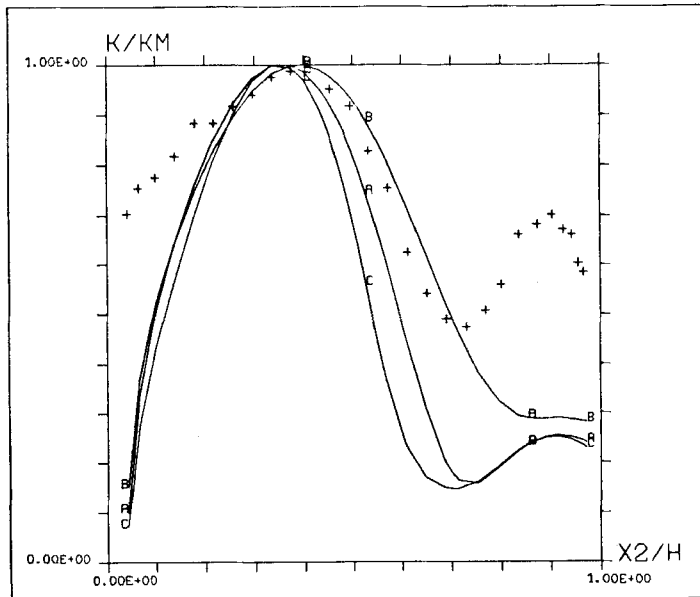Figure 5

Figure 6
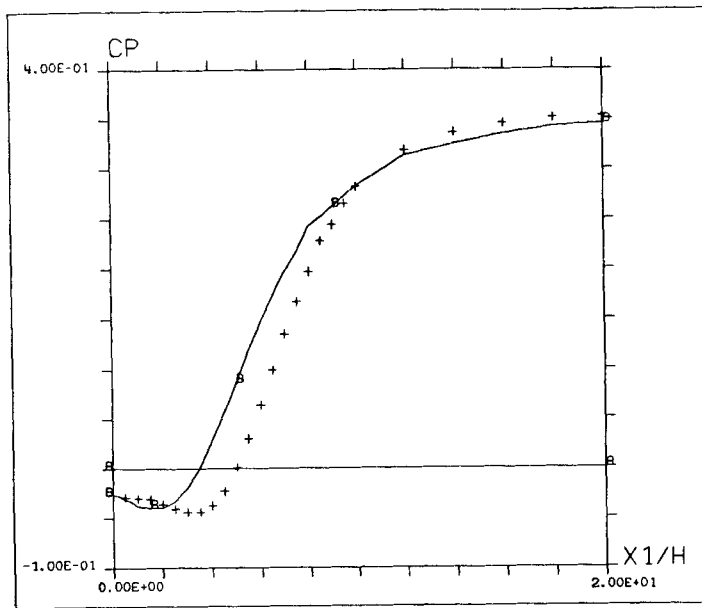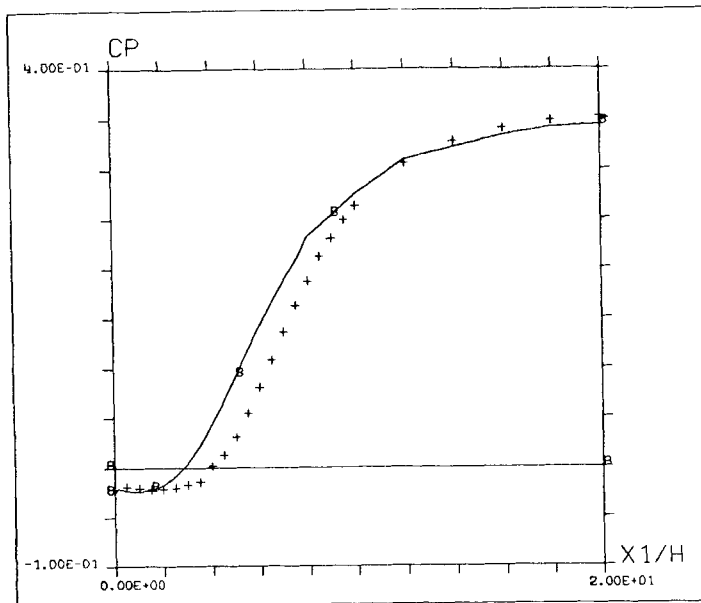

Figure 7

Figure 8

Figure 9

Figure 10

Figure 11

that the predictions of the standard model are not much better in the middle area, but levels are in a better agreement in the jet region. However, the standard model does not predict the second peak, which is qualitatively quite important. Except for this, the locations of minima and maxima are well predicted. Finally the great similarity in the behaviour of the turbulent field between the modified model and the model with variable c_μ should be noted with interest.

Pressure field

Figures 10 and 11 show comparisons between predicted $(c_\mu = 0.045)$ and experimental values of the pressure coefficient

$$c_P = \frac{P - P_{ref}}{\frac{1}{2} \rho U_{ref}^2} \tag{30}$$

along the lower and upper walls. Locations of maximum and minimum c_P are in good agreement and the behaviours of the two curves are very similar. The slight discrepancy along the x_2-axis does not alter the value of the pressure loss.

CONCLUSIONS

The previous section has considered the numerical prediction of a turbulent flow over a two-dimensional backward-facing step by a Galerkin finite element method. The present numerical investigations have proved that the GFEM is a very faithful numerical treatment which exactly reflects the physical phenomena when it is implemented and exploited in the standard manner. In the same way the penalty function approach associated with a turbulence model reveals itself to be as accurate as in the laminar case.

As far as the mathematical model is concerned, we have highlighted its accuracy when it is associated with physical arguments. This last point becomes a very important obstacle in the case of an industrial use of the code. For example, it has been shown how the numerical reattachment length is underpredicted; this could be very prejudicial in the case of thermal problems. In the isothermal case this fault can be corrected with an appropriate choice of c_μ. Finally the use of an analytical formula which relates c_μ to local turbulence parameters is very useful and gives qualitatively better results.

REFERENCES

1. C. Taylor, C. E. Thomas and K. Morgan, 'Modelling flow over a backward-facing step using the F.E.M. and the two-equation model of turbulence', *Int. j. numer. methods fluids*, **1**, 295–304 (1981).
2. A. G. Hutton, 'Current progress in the simulation of turbulent incompressible flow by finite element method', *Proc. 4th Int. Conf. on Numerical Methods in Laminar and Turbulent Flow*, Swansea, 1985, Pineridge Press.
3. W. P. Jones and B. E. Launder, 'The prediction of laminarization with a two-equation model', *Int. j. Heat Mass Transfer*, **15**, 301–314 (1972).
4. M. Bercovier and M. Engelman, 'A finite element for numerical solution of viscous incompressible flow', *J. Comput. Phys.*, **30**, 181–201 (1979).
5. M. Engelman, R. L. Sani, P. M. Gresho and M. Bercovier, 'Consistent versus reduced integration penalty methods for incompressible media using several old and new elements', *Int. j. numer. methods fluids*, **2**, 25–42 (1982).
6. M. Bernard, C. Bouffinier and M. Grandotto, 'Finite element calculation of a turbulent cavity flow', *Int. j. numer. methods fluids*, Submitted for publication.
7. W. Rodi, 'Turbulence models and their application in hydraulics', *Article sur l'état de connaissance*, AIRH, 1980.
8. G. Comte-Bellot, 'Contribution à l' étude de la turbulence de conduite', *Thèse d'Etat*, Université de Grenoble, 1963.
9. A. Autret, 'Calculs d'écoulements turbulents par une méthode aux éléments finis', *Thèse de Docteur Ingénieur*, Université Aix-Marseille II, 1985.
10. R. V. Westphal, J. P. Johnston and J. K. Eaton, 'Experimental study of flow reattachment in a single-sided sudden expansion', *NASA Contractor Report 3765, Report MD-41*, Stanford University, 1984.

11. J. Kestin and P. D. Richardson, 'Heat transfer across turbulent, incompressible boundary layers', *Int. J. Heat Mass Transfer*, **6**, 147–189 (1963).
12. P. L. Betts and V. Haroutunian, 'k-ε modelling of turbulent flow over a backward facing step by a finite element method; comparison with a finite volume solution and experiments', *Proc. 4th Int. Conf. on Numerical Methods in Laminar and Turbulent Flow*, Swansea, 1985, Pineridge Press.
13. C. Taylor, T. G. Hughes and K. Morgan, 'A finite element model of one and two equation models of turbulent flow', *Recent Advances in Numerical Methods in Fluids, Vol. 1*, Pineridge Press, 1980, pp. 311–334.
14. M. Lazareff, 'Expériences numériques sur un écoulement turbulent décollé—Analyse des conditions de paroi', *Thèse de Docteur Ingènieur*, Université Paris VI, 1980.
15. W. Rodi, 'On the equation governing the rate of turbulent energy dissipation', *Ph.D. Thesis*, University of London, 1972.